Chapter 2

The Development of High-Field /High Frequency ESR

Historical overview

Jack H. Freed

Baker Laboratory of Chemistry and Chemical Biology, National Biomedical Center for Advanced ESR Technology (ACERT), Cornell University, Ithaca, NY 14853 USA

Abstract: We discuss the development of high field ESR into a powerful and flexible tool for studies of structure and dynamics in a wide variety of systems including those of biological interest. A range of techniques are discussed with particular emphasis on the developments at Cornell University, but the contributions of other groups to the constant refinement of the state of the art are also noted.

1. EARLY HISTORY

One of the most important instrumental advances in ESR has been its extension to high magnetic fields and high frequencies (HFHF) corresponding to the mm.-wave region.[1-4] While there had been previous use of far-infrared (FIR) spectroscopy that included applied magnetic fields in solid state physics,[5-7] modern HFHF ESR with high SNR and high spectral (and magnetic field) resolution was introduced by the research group of Ya. Lebedev in Moscow.[1,8] Their 150 GHz spectrometer (operating at 5.4T) corresponding to 2mm. wavelength involved sophisticated application of microwave technology, (e.g. waveguides and cavity resonators). This pioneering tour-de-force took high sensitivity, high-resolution ESR to the maximum frequency where microwave technology could sensibly be used. Many useful applications of HFHF ESR were presented by Lebedev and his group during the decade of the '80's,[1] and they are reviewed in Chapter 1.

FROM:
Biological Magnetic Resonance
Vol. 22, Very High Frequency (VHF) ESR/EPR
Edited by: Oleg Grinberg and Lawrence J. Berliner
Kluwer Academic/Plenum Pub. 2004

2. QUASI-OPTICS

The question remained how to take high resolution ESR to higher fields and frequencies. Freed and co-workers showed that the answer lay with the use of mm-wave quasi-optical technology, when they reported on a 9T, 250 GHz (i.e. 1.2 mm) HFHF ESR spectrometer.[2,9] This is in the "near-millimeter" range (i.e. wavelengths from 2-0.1 mm), which corresponds to the long-wavelength end of the FIR regime. [The Grenoble group was meanwhile extending the simpler solid-state type of FIR technique, referred to above, to the higher magnetic fields.[10]] Quasi-optics refers to the fact that at FIR frequencies, one uses techniques that are a natural extension downward in frequency from optical techniques. Quasi-optics thus applies when a geometrical optics description, valid at visible wavelengths, no longer applies. Geometrical optics corresponds to a ray description of radiation that ignores its wave-like properties, (e.g. point focus and non-diffracting beams). In the FIR, where wavelengths are ca. 1mm, and with optical structures having linear dimensions of a few cm, geometrical optics is no longer valid. In fact, diffraction plays a crucial role in the system behavior. This is described, to a good approximation, by Gaussian beams, which are modified plane waves whose amplitude decreases as one moves radially away from the optical axis.[11,12] The simplest, or fundamental, Gaussian beam has a $exp\left(-\rho^2/w^2\right)$ radial dependence, where ρ is the radial distance from the optical axis and w is the position-dependent 1/e radius of the electromagnetic field.[12] The phase of a Gaussian beam also differs from that of a plane wave due to diffraction effects. Further discussion of Gaussian beam propagation appears in Chapter 11 and references therein.

3. QUASI-OPTICAL TRANSMISSION SPECTROMETER

The original 250 GHz ESR spectrometer of the Freed group is a transmission mode design, wherein a quasi-optical lens train was used to propagate the beam from source to Fabry-Perot resonator and then on to the detector, cf. Figure 1.[2,9] The quasi-optical lens train mainly consisted of a series of longer (4.5 inch) focal length primary lenses that refocus the diverging beam and thereby propagate the beam over substantial distances. This method of propagation is much more efficient than that of waveguides; the loss incurred by the lenses over a 54-inch path length is only 2dB, whereas the theoretical loss of WR-4 waveguide over the same distance is 16dB. Also, quasi-optical feedhorns in conjunction with focusing lenses are used to launch the linearly polarized beam from the source and to collect the beam into the detector. Similarly, the radiation is coupled into and out of the Fabry-Perot resonator with two conical feedhorn/focusing lens pairs. The Fabry-Perot resonator was semi-confocal (to

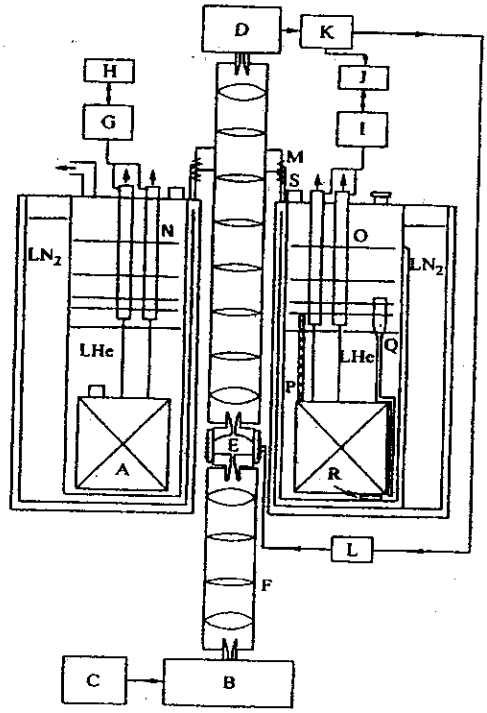

Figure 1. Block diagram of a 1 mm EPR spectrometer, (A) 9 T superconducting solenoid and 500 G sweep coils; (B) phase-locked 250 GHz source (output power 2 mW); (C) 100 MHz reference oscillator for 250 GHz source; (D) Schottky diode detector or InSb hot electron bolometer; (E) Fabry-Perot semiconfocal resonator and field modulation coils; (F) 250 GHz quasioptical lens train; (G) power supply for main coil (100 A); (H) current ramp control for main magnet; (I) power supply for sweep coil (50 A); (J) PC which controls field sweeps of both the main coil and the sweep coil, data acquisition, and data manipulation; (K) lock-in amplifier using DSP technology for signal amplification and detection as well as reference frequency and field modulation generation; (L) field modulation amplifier; (M) support table for detector or InSb hot-electron bolometer; (N) vapor-cooled leads for main solenoid (nonretractable); (O) vapor-cooled leads for sweep coil (nonretractable); (P) ^{4}He bath level indicator; (Q) ^{4}He transfer tube; (R) bath temperature/bath heater resistance pod; (S) ^{4}He blow-off valves. [From 9]. The figure legend has been updated to reflect improvements to the original spectrometer).

permit placing a sample on the flat bottom mirror) with a mode-number, ν=20, (i.e. approximately the number of half-wavelengths between the mirrors) and provided with coupling holes located at the centers of both mirrors. One tunes

the FP to the precise resonance frequency of the source (249.9 GHz) by tuning the distance between the two mirrors. For such a multi-mode resonator, the $Q_L=fv$, where the finesse $f=\lambda/\Delta\lambda$ with λ the tuning length between successive modes, and $\Delta\lambda$ is the full width at half maximum of a single resonator mode. [Möbius and co-workers have also used a FP resonator in their microwave-based ESR spectrometer at 94 GHz.[13]] More extensive discussion of FP resonators may be found in Chapter 11.

The superconducting magnet used provides up to 9.4 T and is sweepable, requiring a relatively low inductance. It has homogeneity of 3 ppm over a sphere of 1 cm radius. In addition, a lower inductance superconducting sweep coil provides more rapid sweeping over about 0.1T.

Subsequent improvements of this transmission mode design led to a very high sensitivity spectrometer where $MN_{min} \cong 1.5\times10^7$ spins/G.[11,14] Here $M\equiv\Delta B_{mod}/\Delta B_{pp}$, where ΔB_{mod} is the modulation amplitude and ΔB_{pp} is the peak-to-peak derivative linewidth of the broadest feature. For an $M\approx1/8$ this corresponds to an $N_{min}\cong1\times10^8$ spins/G. These sensitivity figures were obtained from a spectrum from 6 oriented spin-labeled muscle fibers (radius ca. 10 μm) containing at most 3×10^{10} spins with a $\Delta B_{pp}\approx40$ G using an InSb hot electron bolometer[15] and 80 kHz field modulation. It is close to the optimum expected with the transmission design and using InSb bolometer detection (*cf.* below).[11] Similarly low values were obtained by Lebedev[1] at 150 GHz using microwave technology. The frequency dependence of the sensitivity depends on the details of the sample and whether absolute or concentration sensitivity is relevant. This is addressed from several points of view in Chapters 1, 8 and 11 and below. In homodyne operation, hot electron bolometers perform significantly better as detectors than Schottky diode detectors.[16,17] especially when the background power can be suppressed as in the shunt resonator discussed below, but their response times are too slow for pulse experiments.

4. SIGNAL-TO-NOISE CONSIDERATIONS

What then are the applications and virtues of HFHF-ESR? Clearly, the increase in absolute sensitivity is very important. Earle et al, in their analysis of FIR-cw ESR spectrometers obtained:[11]

$$MN_{\min} \propto \frac{V_s T_s}{\eta Q_L P_0^{1/2}} \left(\frac{\Delta\omega_{PP}}{\omega} \right) \propto \omega^{-1} V_s \eta^{-1} \frac{\Delta\omega_{PP}}{Q_L} \qquad (1a)$$

or $$M\left(N/V_s\right)_{min} \propto \omega^{-1}\eta^{-1}\frac{\Delta\omega_{PP}}{Q_L} \qquad (1b)$$

where ω, V_s, η, Q_L, and P_0 respectively are the spectrometer frequency, the sample volume, the filling factor, the loaded Q or quality factor, and the incident

power, while $\Delta\omega_{PP} = \gamma_e \Delta B_{PP}$ and T_s is the sample temperature. This predicts a linear increase with ω of both absolute and concentration sensitivity, provided the technology remains unchanged. The actual situation is not quite so simple. Thus, as ω and B_0 increase, $\Delta\omega_{PP}$ is in most (but not all) cases observed to increase, thereby acting to reduce sensitivity. Also, as $\Delta\omega_{PP}$ increases, it becomes more difficult to provide sufficient modulation amplitude (ΔB_{mod}), so that M decreases, which further reduces the actual sensitivity. In addition, given the smaller wavelengths, one usually works with smaller samples, especially if they are lossy, implying that one may have to be operating closer to the N_{min}. Thus, methods to overcome the small values of M and/or to load up more sample into the high-frequency resonators would be of considerable value. Also, higher power levels at the FIR frequencies from stable cw sources are highly desirable (*cf.* below).

5. APPLICATIONS TO MOLECULAR DYNAMICS IN FLUIDS

IMPROVED ORIENTATIONAL RESOLUTION: One of the main virtues of FIR-ESR over ESR at conventional microwave frequencies is the excellent orientational resolution that it provides for studies utilizing nitroxide spin labels.[2,18-20] This is clearly shown in Figure 2, which shows the positions of the resonant ESR absorptions for the canonical orientations of a typical spin probe in a powder simulation at 9.1 and at 250 GHz. At 250 GHz the regions corresponding to molecules with their x-axis $\| B_o$, y-axis $\| B_o$, and z-axis $\| B_o$ are well separated due to the dominant role of the g-tensor. This is definitely not the case at 9.1 GHz. As a result, at 250 GHz, once motion is discernible in the spectrum, one can discern about which axis (or axes) the motion occurs. Thus, Earle et al[18] were able to demonstrate that the 250 GHz slow-motional spectra are much more sensitive to the details of the motional dynamics than are those at microwave frequencies, (cf. Figure 3). The improved orientational sensitivity is also important in enabling "single-crystal"-like ENDOR to be performed on powder samples, as described in Chapters 3, 10 and 14.

MODEL DEPENDENCE IN FAST AND SLOW MOTIONAL REGIMES: A related important feature of the 250 GHz studies is the ability to measure very accurately from (near) rigid limit spectra, the magnetic tensors needed for the motional studies.[2] Especially given these capabilities, Budil et al showed that one can use 250 GHz ESR spectra of nitroxides in the motional narrowing regime to obtain the full anisotropic diffusion coefficient for the molecular tumbling motion.[21] In fact, it was the increased sensitivity of 250 ESR to the details of the motional dynamics, that originally motivated the extension of the sophisticated slowly-relaxing local structure (SRLS) model to the slow-motional regime.[22] In the earlier analyses of slow-motional ESR lineshapes using the

stochastic-Liouville equation (SLE), simple Markovian models were employed that just distinguish between reorientations by large, moderate, or small (i.e. Brownian) jump diffusion.[18,23] However useful these models were in fitting spectra, they beg the issue of the details of the interaction of the probe molecule with the solvent molecules. The SRLS model provides in a relatively simple manner, the essential features of a loose solvent "cage" that had been absent from the earlier models,[19] but it does require increased computational efforts. Computational issues in using the SRLS model are discussed in Chapter 4 and references therein.

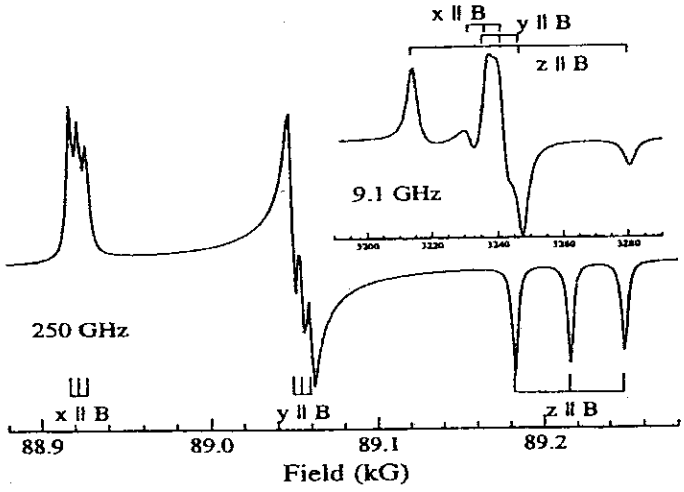

Figure 2. Simulation of derivative electron spin resonance spectra at 9.1 and 250 GHz for dilute powder containing a cholesterol-like nitroxide (CSL). The fields where CSL absorbs when its x', y', or z' axes are parallel to B_0 are indicated by the short vertical lines. The hyperfine interaction splits the absorption at the spectral turning points into triplets. [From 32].

Another key feature of the 250 GHz ESR spectra is that the slow-motional spectral regime is reached for motions that are about an order of magnitude faster than for conventional 9 GHz ESR.[18] This is associated with the faster "snapshot" feature of 250 GHz ESR discussed below. However, this means that a slow-motional analysis is more frequently required for HFHF-ESR spectra. Thus although a simplified "quasi-motional-narrowing" form of analysis, discussed in Chapter 13, is sometimes used, it is advisable to check whether it is at all valid in a particular application by comparison with the rigorous slow-motional theory based on the SLE. In fact it was shown some time ago for 9 GHz ESR[24] that nitroxide ESR spectra, especially in ordered media (e.g. membranes and liquid crystals), frequently require a slow motional analysis even when their spectral line shapes might intuitively suggest that a fast-motional analysis is appropriate. In such cases incorrect dynamic and ordering parameters are obtained from the simpler fast-motional analysis. This becomes an even more serious matter for HFHF-ESR, where, as we noted, the slow-motional regime extends to faster motions. This matter is important

for experimental studies of dynamics discussed in Chapters 3, 4, 8, and 13.

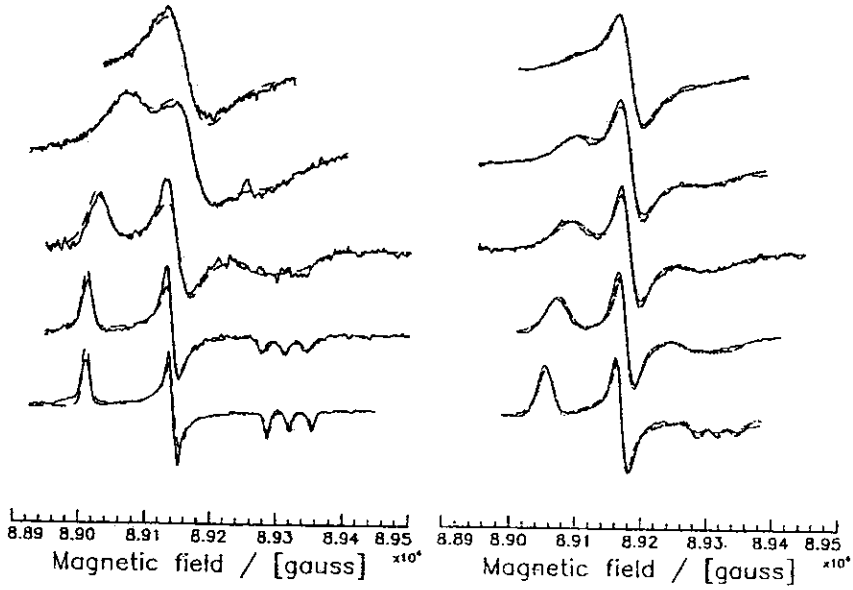

Figure 3. (a, left) Selected slow-motional 250-GHz EPR spectra of PDT in toluene-d8 (solid lines) at temperatures of (top to bottom) -97, -107, -118, -128, and -134°C. Dashed lines show least-squares spectral fits for approximate free diffusion with τ_R values (from top to bottom) of 4.2×10^{-10}, 1.2×10^{-9}, 3.4×10^{-9}, 1.5×10^{-8}, and 3.5×10^{-7}s.(b, right) Slow-motional 250 GHz EPR spectra of CSL in toluene (solid lines) at temperatures of (top to bottom) -86, -92, -97, -106, and -116°C. Dashed lines show least-squares fits to Brownian diffusion and dotted lines those for the mixed diffusion model described in ref. 18. From top to bottom, τ_R values for the mixed model are 1.6×10^{-9}, 2.5×10^{-9}, 5.0×10^{-9}, 7.9×10^{-9} and 2.5×10^{-8}s [From 18].

DYNAMIC SOLVENT CAGE AND SLOWLY RELAXING LOCAL STRUCTURE MODEL: In a 250 GHz ESR study of the dynamics of several nitroxide spin probes dissolved in the glass-forming solvent ortho-terphenyl, (OTP), Earle et al demonstrated how the enhanced sensitivity to rotational dynamics of the slow-motional spectra could be utilized to explore details of the dynamic solvent cage.[19] They clearly showed that a simple Brownian reorientational model failed to adequately fit the model-sensitive regions of the 250 GHz spectra, whereas the SRLS model succeeded very well (cf. Figure 4), and in fact, led to a coherent picture of the dynamics that I briefly summarize. The rotational diffusion tensors of the various probes exhibited simple Arrhenius behavior such that the smaller the probe the larger the diffusion coefficient. The cage relaxation rate, also Arrhenius-like, was the slowest but was independent of the particular probe. This interesting observation appears reasonable when one considers that

the cage relaxation involves just the movement of the OTP solvent molecules. In addition, the magnitude and directionality of the cage orienting potential could be obtained. As expected, only probes comparable to or larger than the OTP molecules experienced substantial potentials, of 2-4 kT. This work was also relevant for issues related to the approach to the glass transition. It was possible to show that the non-linear way in which the dynamics affects the slow-motional spectra yields a test of two limiting cases. The first is that of a homogeneous liquid but with a complex motional dynamics, (e.g. the SRLS model). The second is that of an inhomogeneous liquid with a distribution of simple relaxation times, (e.g. Brownian tumbling). The latter was shown to be incompatible with the 250 GHz spectra.

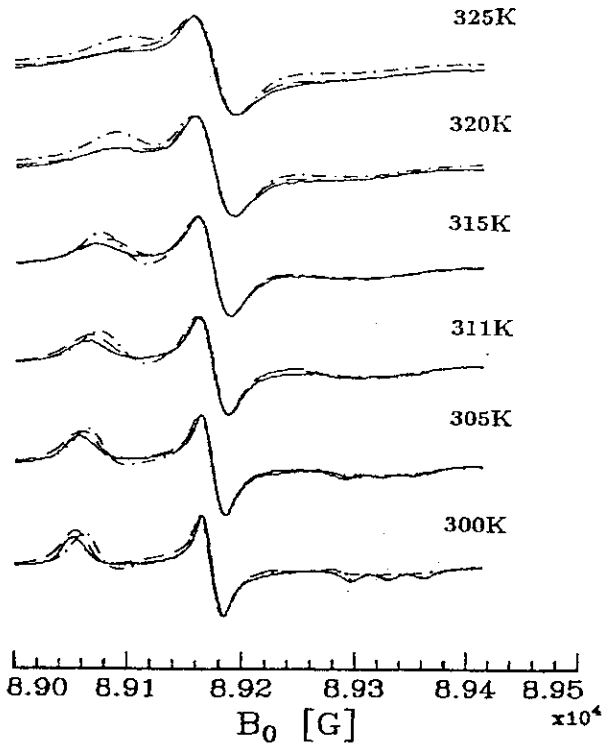

Figure 4. Comparison of two models for fitting effects of rotational diffusion on 250 GHz electron spin resonance spectra of spin probe of a cholesterol-like nitroxide (CSL) in ortho-terphenyl solvent. (Solid line) Experiment, (dashed line) the SRLS model, and (dashed-dotted line) simple Brownian diffusion. [From 19].

HIGH FREQUENCY ESR AS A FASTER "SNAPSHOT" OF MOLECULAR DYNAMICS: Another virtue of FIR ESR is the fact that the higher the ESR frequency, the slower the motion appears to be for a given diffusion rate. This is illustrated in Figure 5 where I show simulated spectra

corresponding to the same motional rate but for different ESR frequencies ranging from 15 GHz to 2 THz. At the low frequency end, one observes simple motionally narrowed spectra whereas, at the high frequency end, the spectra are very slow motional, almost at the rigid limit. Thus we see that the higher frequency ESR spectra act as a faster "snapshot" of the dynamics.[18,19] This is because of the increased role of the g-tensor term which is linear in B_o in the spin-Hamiltonian. As the orientation-dependent part of the spin-Hamiltonian $H_1(\Omega)$ increases in magnitude with increasing ω_o and B_o, the motional-narrowing condition: $|H_1(\Omega)|^2 \tau_R^2 << 1$ fails, and the spectra become slow-motional. This "snapshot" feature is discussed below, as well as in Chapters 13 and 15.

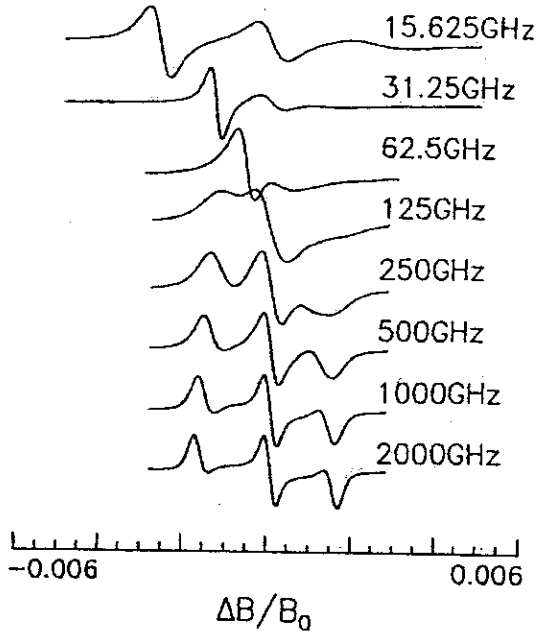

Figure 5. Simulation of derivative electron spin resonance spectra for a nitroxide, reorienting with a rotational diffusion coefficient R = 108 s-1 (corresponding to rotational correlation time τR = 1.67 ns) for a wide range of frequencies [From 3].

MULTI-FREQUENCY APPROACH TO COMPLEX DYNAMICS OF FLUIDS AND OF MACROMOLECULES: This "snapshot" feature suggests a multi-frequency ESR approach to the study of the dynamics of complex fluids such as glass-forming fluids and liquid crystals, as well as to the complex modes of motion of proteins and DNA, which should enable one to decompose the different modes according to their different time scales.[25] For

example, in the case of proteins, the higher frequency ESR spectra should "freeze-out" the slow overall tumbling motions leaving only the faster internal modes of motion, whereas ESR performed at lower frequencies is sensitive to the motions on a slower time scale. In glass-forming fluids, as we have seen, the faster motions consist of reorientations of probe molecules, while the slower motions relate to the dynamics of the solvent cage. Ideally then, one would want a high-sensitivity spectrometer for the study of fluids that could cover a wide range of frequencies to most effectively realize such a multi-frequency approach. The virtues of such a multi-frequency approach were demonstrated in a study, using 9 and 250 GHz spectrometers, on spin-labeled mutants of the soluble protein T4 lysozyme in aqueous solution, (cf. Figure 6).[26]

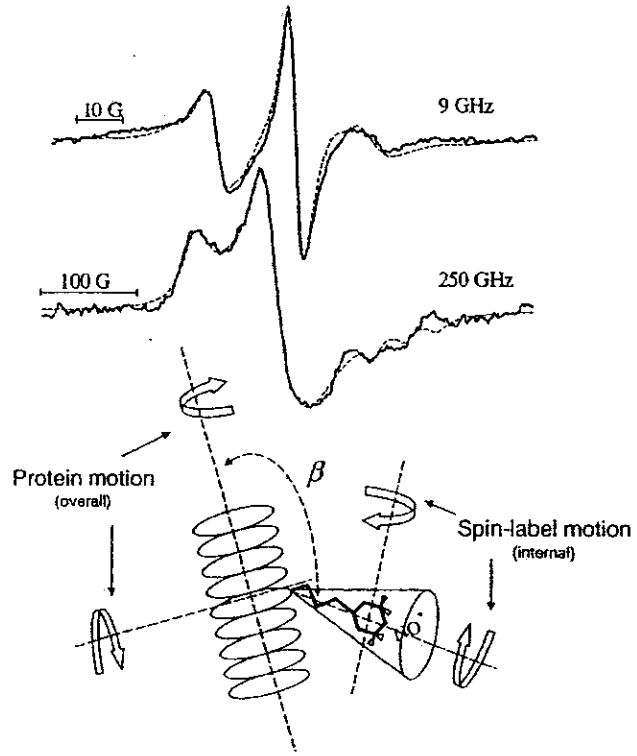

Figure 6. A multifrequency ESR study of nitroxide spin-labeled T4 lysozyme in aqueous solution. The derivative spectra are for the spin label on residue 44 and are taken at 10°C. The relevant molecular motions are shown schematically in the lower part of the figure. The protein tumbles slowly about its principal axes of overall diffusion; this is the SRLS. The motion of the spin label moiety is restricted by its tether and its surroundings to be within a cone, whose main axis makes an angle β with the protein main axis. The spatial extent of the internal rotational diffusion modes and their rates are distinguished from the protein overall tumbling rates. [From 4].

In the fast time scale of the 250 GHz ESR experiment, the overall rotation was too slow to significantly affect the spectrum, so that it could satisfactorily be described by a MOMD model, which yielded good spectral resolution for the internal dynamics. Then, by fixing the internal motional parameters at the values obtained from the 250 GHz data, the SRLS fits to the 9 GHz lineshapes successfully yielded the rates for the global dynamics. Thus the two types of motion were separated, and spectral resolution to these motions was significantly enhanced.

In a related 9 and 250 GHz study of segmental rotation of spin labeled polystyrene in dilute solution, Pilař et al found systematic discrepancies between the 9 and 250 GHz results when they were separately fit by the MOMD model.[27] This observation is exactly what Barnes et al observed in their Lysozyme study,[26] suggesting that the discrepancies can again be resolved by using the SRLS model for analyzing the 9 GHz results.

In another study of DNA oligomers covering a range of sizes that were spin-labeled with nitroxide moieties attached by different tethers, the SRLS model was successfully utilized.[28] Given that only the 9 GHz spectra were available, the global dynamics was fixed at the values obtained from well-established hydrodynamic theory. These authors note that more reliable insights would likely be obtained from a multi-frequency approach. Additional HFHF work on proteins and peptides in aqueous solution can be found in the work of Budil,[29] Millhauser,[30] and Smirnov.[31]

A multi-frequency approach has also been found very useful in solid-state ENDOR studies, as described in Chapters 3, 9 and 14.

COMBINING ORIENTATIONAL RESOLUTION AND MACROSCOPIC SAMPLE ALIGNMENT: MEMBRANE DYNAMICS: A striking demonstration of the value of having excellent orientational resolution at 250 GHz in studies utilizing nitroxide spin labels was provided by a study on macroscopically aliigned membranes containing a mixture of headgroups: zwitterionic phosphatidylcholine (PC) and negatively charged phosphatidylserine (PS) using the cholesterol-like spin label CSL.[32] The macroscopic alignment further enhanced the orientational resolution at 250 GHz and permitted an orientation-dependent study wherein the membrane normal could be aligned either parallel or perpendicular to the magnetic field (cf. Figure 7a and below). The CSL in PC rich membranes exhibited typical cholesterol-like behavior, such that its long axis is parallel to the bilayer normal and its rotational diffusion rates are slow ($R \sim 10^6 - 10^7\ s^{-1}$). But it exhibits markedly different behavior in PS rich membranes that can only be interpreted in terms of a strong local biaxial environment. The origin of the biaxiality is most likely due to the strong ferroelectric interactions between the PS headgroups that provides the local biaxiality. This local biaxiality provides a void that allows the CSL to "cut" into the hydrocarbon chain region of the bilayers by reorienting about its broad face. While predicted from molecular dynamics simulations, this appears to be the first experimental evidence for local biaxiality. By contrast,[32] given the poor orientational resolution at 9.1 GHz, it would not have been possible to

obtain this unique motional/ordering model from the 9.1 GHz experiment. The orientational resolution from HFHF ESR is useful even for membrane vesicles.[2,33,34]

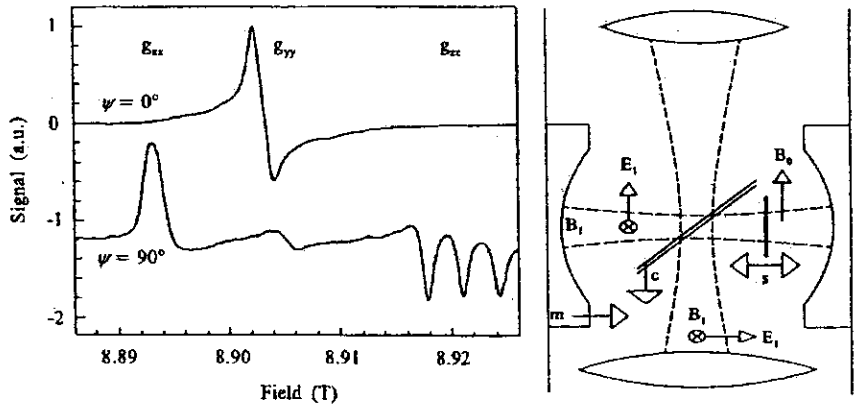

Figure 7. (left) Gel phase spectra of CSL in a macroscopically aligned phospholipid membrane showing the superior orientational resolution of HFEPR. (right) The relative orientations of the millimeter-wave fields in a shunt resonator (From 51).

Another application of a multi-frequency approach was to determine the ZFS of high-spin Gd(III) chelates in aqueous solution using the field-dependence of the dynamic frequency shift and the T_2 that arise from modulation of the ZFS.[35] Studies of systems with large ZFS parameters in the solid state are reported in Chapter 5. Chapter 7 discusses the Gd(III) chelate problem from a theoretical and practical point of view motivated by their widespread use as MRI contrast enhancing agents.

6. ENHANCEMENT OF SPECTRAL RESOLUTION

Further motivation for the development of HFHF ESR comes from the resolution enhancement it can provide. This includes the ability to resolve signals from components that differ only slightly in their g-tensors. Examples include electrides and alkalides in frozen matrices[36]; resolution of thiyl radical in *E. coli*[37]; spin adducts for spin trapping[38]; and resolution of the *g*-tensor of the radical pair P(700)(.+)A(1)(.-) in highly purified photosystem.[39] These are cases where at X-band the different components or species are not distinguishable, nor are their g-tensors resolvable. Additional cases where g-tensors become

observable include the polyaniline family of conducting polymers[40] and various coal samples.[41] A particularly useful application in biological samples is the sensitivity of the g_{xx} component of nitroxides to the local polarity. Earle et al[42] were able to demonstrate that large shifts of g_{xx} occurred in frozen membrane vesicles as the nitroxide moiety was located at different positions on the hydrocarbon chain of the lipid, with g_{xx} decreasing as the local polarity increases (cf. Figure 8).

Earlier work of Ledeev[1] had also revealed the sensitivity of the nitroxide g-tensor to the "micro-environment". Polarity effects on g_{xx} are also discussed in Chapter 3.

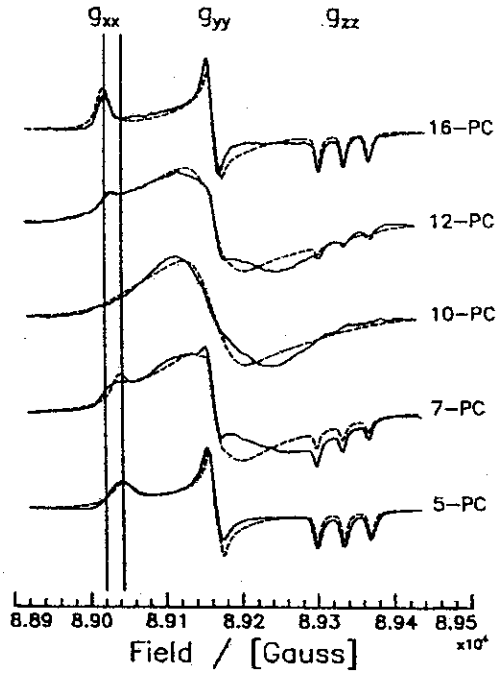

Figure 8. Rigid limit 250-GHz spectra of 5-, 7-, 10-, 12-, and 16-PC in pure DPPC (hydrated). Simulations of the spectra are shown by dotted lines for 5-, 7-, 12-, and 16-PC. They yielded g_{xx} = 2.00869, 2.00873, 2.00880, and 2.00929 respectively. The vertical lines indicate the shift of the g_{xx} peak as the label environment changes from non-polar (16-PC) to polar (5-PC). [From 42].

7. TRANSITION-METAL IONS

Another key application of HFHF ESR is to the study of transition-metal ions. A particularly useful special case is with ions, such as Mn(II) in its high spin ^5S state, with rather large zfs (up to ca. 1 cm^{-1}) and small (or negligible g-tensors). In such cases the low-field ESR spectra are usually complicated, since the Zeeman interaction is smaller (or comparable to) the zfs. However, it is found that at high fields the ESR spectra are quite simple and can be very easily interpreted to extract the zfs tensor (cf. Figure 9).[43,44]

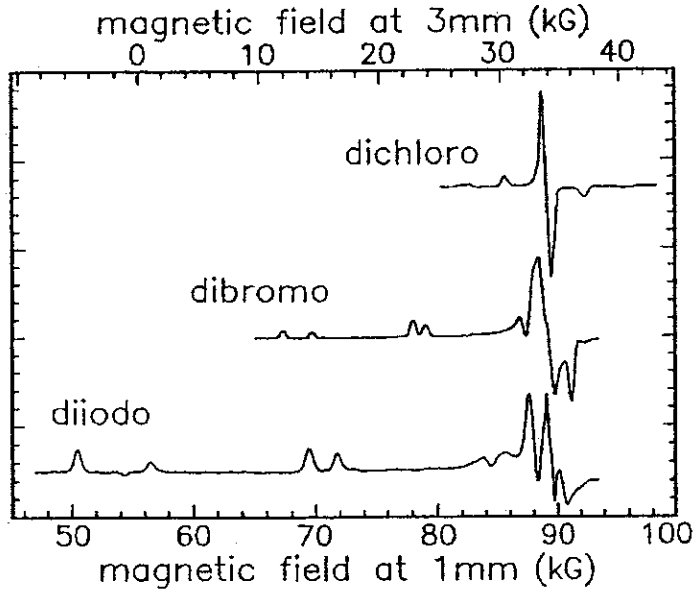

Figure 9. Example showing that high magnetic fields and high frequencies yield simple electron spin resonance (ESR) spectra from transition metal ions with large zero-field splitting (zfs). High-field ESR spectra of Mn(II) in distorted tetrahedral environments. These are the dihalo-(trihenylphosphine oxide) Mn(II) complexes. The zfs are 4.8, 15.3, and 27.3 GHz for dichloro, dibromo, and diiodo complexes, respectively. The dichloro spectrum is at 95 GHz; the other two are at 250 GHz [From 44].

In addition, non-Kramers ions, such as Ni^{2+} pose serious problems of detection at lower frequencies, and HFHF represents an important tool to study them.[45-47] Such experiments typically require that one sweep the main superconducting magnet over several Tesla.

In general, transition-metal ions have substantial g-tensors. Consequently, when one goes to higher fields, there will be significant g-tensor broadening in disordered solids, which will tend to obscure other features. Such problems are exacerbated by the existence of g-strain. Clearly single-crystal studies are

required to suppress this source of broadening. A single crystal study at 250 GHz has been performed on Ni^{2+} doped $CdCl_6$ where the Ni^{2+} ions are octahedrally co-ordinated with 6 H_2O molecules.[14,48] This yielded very simple and easy to interpret spectra with two species, (cf. Figure 10a) one showing a large (almost 1 cm^{-1}) and the other a small (about 1/5 cm^{-1}) zfs, but this is again a case of a (nearly) isotropic g-value.

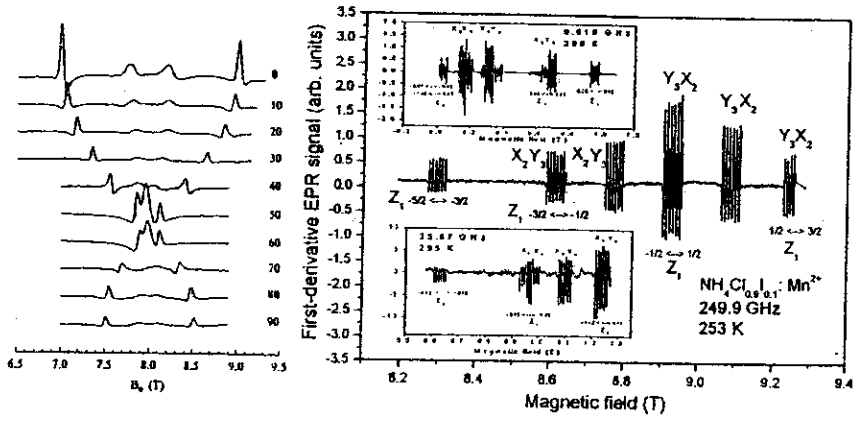

Figure 10. (left) A set of spectra corresponding to a crystal rotation study of Ni-doped CdCl6. The orientation of the crystallographic c-axis with respect to the external magnetic field B0 is shown to the right of the spectrum in degrees. (From 14). (right) Observed EPR spectra of the Mn^{2+} ions in the $NH_4Cl_{0.9}I_{0.1}$ single crystal at 249.9 GHz (253 K) for $B\|Z_1\|X_2\|Y_3$ axes. (The subscripts refer to the three magnetically inequivalent ions.) The clearly resolved lines belonging to the three magnetically inequivalent ions are indicated by Z_1, X_2, Y_3 for $B\|Z_1$ at 249.9 GHz. The fine-structure transitions corresponding to hyperfine sextets are indicated. The expected lines above 9.3 T are not observed at 249.9 GHz because 9.3 T is the upper limit of the magnetic field available at this frequency. It is seen that the FIR spectrum at 249.9 GHz provides considerable simplification of the spectrum allowing one to easily distinguish the EPR lines belonging to the three magnetically inequivalent ions. The insets show corresponding EPR spectra at X (9.619 GHz, 295 K) and Q (35.87 GHz, 295 K) bands, [From 49].

A recent dramatic demonstration of the resolution of single crystal studies is shown in Figure 10b.[49] Some other examples include binuclear Mn(III) Mn(IV) complexes,[45] Mn(III) compounds,[46] and Cr(II).[47] These applications are extensively discussed in Chapters 5, 10, and 14.

8. QUASI-OPTICAL RESONATORS AND SAMPLE HOLDERS FOR LOSSY (AQUEOUS) SAMPLES

In the development of HFHF ESR, certain sample characteristics provided challenges that required the development of appropriate quasi-optical solutions. Most critical is the problem of lossy samples such as aqueous (including biological) samples and the highly conducting alkalides and electrides as well as the polyanilines. Barnes and Freed analyzed this matter in detail for confocal Fabry-Perot resonators.[50] They found that a flat, disk-shaped sample geometry is required to simultaneously maximize the resonator filling factor and Q by minimizing dielectric losses in the sample. The FP resonator must have provision for precisely locating the flat sample at a B_1 maximum and E_1 minimum near the center of the resonator with its normal parallel to the main symmetry axis of the FP resonator. At 1.22 mm (250 GHz) the optimum thickness of an aqueous sample is only 10-25 μm. For such small sample sizes, volumes less than 1 μL are sufficient to fill the holder, and a high spectrometer SNR is required. Clearly, the sample holder material should have low dielectric losses and be resistant to attack by the sample. This includes very thin (ca. 0.1 mm) discs of Mylar and fused silica.[50] A useful method for evaluating optimum resonator configurations for lossy samples is given in Chapter 11.

A more sophisticated challenge arises when oriented membranes are studied, and one wishes to tilt such lossy samples relative to the direction of the magnetic field. Barnes and Freed[51] found a special quasioptical design for handling such samples, that they call a shunt FP resonator. In particular, they used a tilt of 90°, as shown in Figure 7b (shown above). The disc shaped aqueous sample must still be kept in the B_1 maximum and E_1 minimum. Thus the confocal FP resonator is oriented so that its main axis is perpendicular to the incident (and exiting) beams of FIR radiation. The coupling between the (vertical) transmission beam and the (horizontal) beam mode in the FP is accomplished with an adjustable interferometer contained within the FP resonator that is tilted at 45° with respect to the main beam. The quasioptical interferometer is constructed from two dielectric sheets, separated by an adjustable small gap.

9. MODERN QUASI-OPTICAL SPECTROMETER BRIDGES

Given the initial successes with a quasioptical transmission mode spectrometer, the question naturally arises as to the optimum design of a quasioptical ESR spectrometer. I have already addressed resonator design and performance, as well as quasioptical transmission techniques. However, microwave-based ESR spectrometers are virtually always based on bridge

systems in a reflection mode. There are a number of well-known reasons for this. A principal advantage is that a reflection-mode bridge can be balanced so that the small ESR signal can be detected on a small background. This is not generally so for the transmission mode; [the shunt resonator provides a special case where it is possible.[51]] A related issue is whether the dynamic range of the detector is sufficient so that the reflected carrier (i.e. non-ESR) signal does not saturate it. This problem is avoided in a well-tuned reflection-mode spectrometer in which the resonator is critically coupled. In addition, the reflection mode of operation is intrinsically more compact and more flexible in terms of the relevant quasioptical elements.

There are at least two possible modes of operating a quasioptical reflection bridge, as depicted in Figure 11.[11,14]

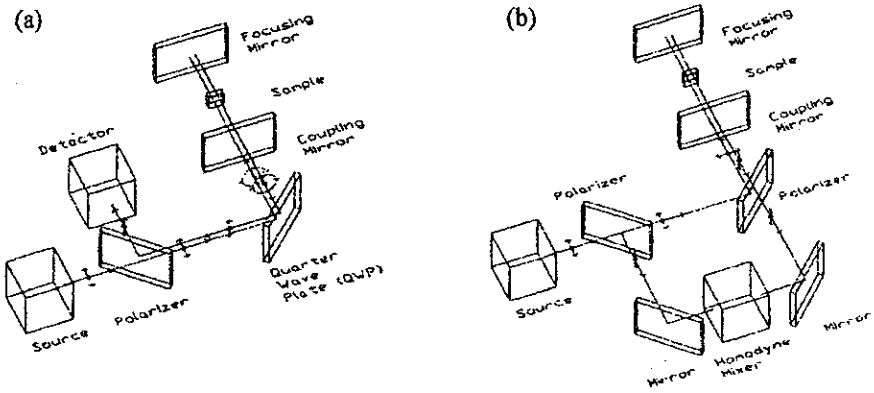

Figure 11. a) A schematic diagram of the reflection bridge discussed in more detail in [52]. The quarter wave plate (QWP) converts horizontally polarized radiation from the source into circularly polarized radiation, which irradiates the spins. The coupling mirror and focusing mirror define the Fabry-Perot resonator used to enhance the B_1 field at the sample. The signal from the resonator, which is circularly polarized in the opposite sense, is converted by the QWP into vertical polarization, causing it to be reflected by the polarizer, directing it to the detector. b) A schematic diagram of an induction-mode reflection bridge with an LO bias arm along the lines discussed in [53]. Here the horizontally polarized radiation from the source is used to irradiate the spins in the resonator. However, only the vertical component of the signal passes through a polarizer and into the detector operated as a homodyne mixer. [From 14].

The scheme shown in Figure 11A has been implemented at Cornell.[52] It is the quasi-optical analogue of a microwave bridge with a circulator, and it showed significant improvement in SNR compared to the transmission mode. It uses polarization coding techniques to separate the ESR signal from the excitation. The quarter wave plate (QWP) converts horizontally polarized radiation from the source into circularly polarized radiation, which irradiates the spins. The coupling mirror and focussing mirror define the FP resonator used to

enhance the B_1 field at the sample. The signal emanating from the FP resonator is circularly polarized in the opposite sense. It is converted by the QWP into vertical polarization, causing it to be reflected by the polarizer, thereby directing it to the detector.

The second mode of operation, shown in Figure 11B is a quasioptical induction-mode spectrometer implemented at St. Andrew's.[53] Here the horizontally polarized radiation from the source is used to irradiate the spins in the resonator. However, only the vertically polarized component of the signal passes through a polarizer, and into the detector that is operated as a homodyne mixer. One relies on the fact that in ESR, the sample's rf susceptibility tensor provides a cross-polarized signal component. Earle et al[14] reported that a polarization isolation of 30dB for the carrier signal is a reasonable estimate. Two new spectrometers at our ACERT Center at Cornell are based on this design. Further discussion of spectrometer configurations and related sensitivity considerations may be found in 11.

These modes of operation clearly show that there is a quasi-optical analogue to the typical designs of microwave spectrometers. The flexibility of the quasioptics enables many variants of these basic designs. The Jones Matrix formalism has proven to be a useful tool for analyzing quasioptical designs and their relationships to equivalent microwave realizations for resonators,[11,54] Also, quasioptical components, such as reflecting mirrors and lenses, can readily be fabricated using standard machine shop practices. This is because the relevant wavelengths are on the order of mm. Given that quasioptical components have diffraction-limited performance,[12] the components will exhibit good optical performance provided that surface tolerances of the order of tenths of a mm. are achieved.

Several groups besides the ACERT group at Cornell are now operating ESR spectrometers based on such quasioptical designs. These include the groups of Brunel,[55] Budil,[56] Möbius,[57] and Smith.[53] Good solid state sources such as phase-locked Gunn oscillators, whose outputs can be frequency multiplied, enable HFHF experiments up to almost 400 GHz (corresponding to 14T sweepable magnets). It is, of course, important to minimize amplitude and phase noise in the sources, a matter discussed further in Chapters 1, 8, and 12. Actually, liquid solution work has been performed using the very low dielectric loss OTP solvent up to 670 GHz with a 25T resistive magnet and an FIR laser.[58] FIR lasers are an appropriate solution for work above 400 GHz, but they are not nearly as convenient to operate as the stable solid state sources. Also, large resistive magnets require major dedicated facilities.

10. OTHER INSTRUMENTAL FEATURES

LIMITATIONS OF MAGNETIC-FIELD MODULATION: As discussed above, a limiting SNR feature of quasi-optical spectrometers is the available

modulation amplitude. In many cases $\Delta B_{mod} << \Delta B_{pp}$, (i.e. $M << 1$). It is probably not practical to use $\Delta B_{mod} > 20$-25G because of sample heating effects. The possibility of using an analogue to the technique of circular dichroism, by using circularly polarized millimeter waves, is being considered at ACERT. The important technique of transient HF-ESR, discussed in Chapters 3, 6, 10 and 14, can be implemented in the direct detection-mode without field modulation.

CURRENT PULSE TECHNIQUES Another approach is to employ pulse techniques, since they remove the need for field modulation. Most HFHF pulse spectrometers to date are limited by the weak coherent radiation sources available for the pulsing.[59-63] Typically pulses are of ca. 20-500 mW intensities, which correspond to $\pi/2$ pulses of ca. 50-100 ns using small single mode resonators at 95-150 GHz. This has proved satisfactory for work at very low temperatures, where relaxation times are very long.[64] Such work is amply described in Chapters 3, 8, 10, 11 and 14. However, for fluids at or near room temperature, these spectrometers are not satisfactory for such purposes. For example, at 250 GHz one can have nitroxide T_2's as short as a few ns. It would be impossible to rotate such electron spins by a $\pi/2$ pulse lasting 50-100 ns. In addition, such long pulses will have very small spectral bandwidths (e.g. about 10 MHz for a 60 ns $\pi/2$ pulse), so only a small fraction of the spins will be irradiated. The question then is how to achieve higher power, preferably coherent, pulses. Griffin has used a gyrotron at 140 GHz to provide a "pump" power of ca 100W in DNP (dynamic nuclear polarization) experiments.[65] For ESR detection, one can use the gyrotron to provide short pulses for FID's.[65] But, since the gyrotron signal was not very clean, then it might be better to use a standard stable low power cw source for detection of, e.g. the spin-inversion recovery, after a gyrotron pulse.[66] There has been some success with the use of FIR lasers at 604 GHz which produced 100ns pulses.[67] Here quasioptical techniques of beam splitting followed by time delay of one of them, can lead to a two (phase coherent) pulse spin echo sequence, but it becomes difficult to step out the pulse separation. Instead, two separate lasers can be used, but one must adjust them to exact resonance, a difficult task.[67] In general, phase coherences between such pulses remain a concern.

DEVELOPMENT OF INTENSE COHERENT PULSE SOURCE FOR 95 GHz: It would seem that the best approach is to use the weak coherent pulses that can be generated with existing solid-state sources, and then amplify them by analogy to pulsed microwave spectrometers. At ACERT we have succeeded with developing a 1 kW pulse source at 95 GHz with $\pi/2$ pulse widths as small as 2.5 – 5 ns.[68] A phase-locked IMPATT oscillator and PIN diode switches provide the 90 mW pulses (with a nominal minimum pulse spacing of 10 ns). They are amplified by an extended interaction klystron amplifier (EIK/A). This system has full quadrature phase cycling capability. The Fabry-Perot resonator that we developed utilizes a novel coupling scheme, which allows one to critically couple to a variety of samples, which is important in maximizing the B_1 and in minimizing spectrometer deadtimes. These are the properties required

to perform pulse and 2D-FT-ESR experiments in fluid media. These high-power pulse source and the FP resonator are used with a quasioptical bridge configured as an induction mode reflection bridge spectrometer to minimize the magnitude of any reflected pulses reaching the detector.[68] It also operates in a heterodyne fashion with a 0.7 GHz IF bandwidth and an IF frequency of 1.82 GHz. This is needed, because Schottky diode detectors, which have fast enough response times to permit ns data acquisition rates, have poor *1/f* noise performance at lower frequencies, especially below 1 MHz. The use of such a high-power pulse source enables one to perform sophisticated experiments. These include 2D-ELDOR experiments, which are especially valuable for studies of molecular dynamics in complex fluids and in biosystems.[3,4] An example of such an experiment, obtained at 95 GHz is shown in Figure 12.

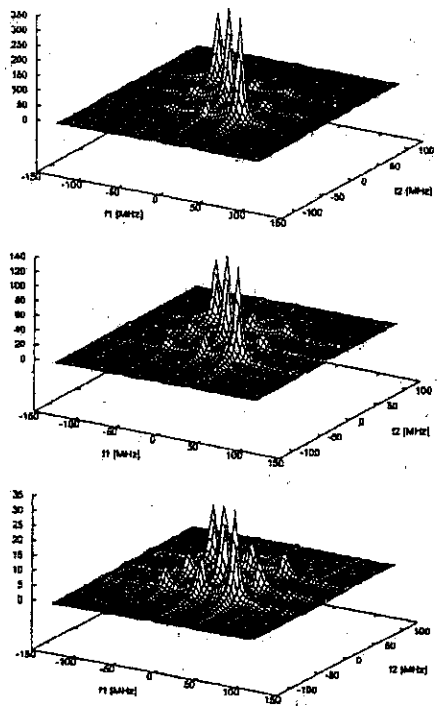

Figure 12. 2D-ELDOR Sc- spectra of TEMPO in decane at room temperature for various mixing times Tm , at 95 GHz. From top to bottom: T_m = 50, 150, and 300 ns. Acquisition time per spectrum is 24 s (430 s for T_m = 300 ns). The growth of the cross-peaks with T_m results from Heisenberg spin-exhange collisions. [From 68].

The EIK/A approach could be extended to 220-250 GHz.[69] Another possibility for a mm. pulse amplifier could be the gyroklystron, (L.C. Brunel, private communication) which is currently being developed,[70,71] Also orotrons

[which are free electron masers based on the Smith-Purcell effect[72]] (K. Möbius, private communication) which supply ca. 50 mW of pulse power, have been developed.

The advent of high power pulsed spin-echo and 2D-EPR at HFHF should combine the excellent orientational resolution and "fast-snapshot times" of this frequency range with the ability to look directly at the spin relaxation processes, e.g. to be able to distinguish homogeneous (T_2^{-1}) line-widths from inhomogeneous line broadening, which proved very useful for studies of complex fluids at microwave frequencies. This may be expected to herald in a new era in the application of ESR to fluids as well as to many other types of samples and objectives.

11. SUMMARY

Modern HFHF ESR has greatly expanded the capabilities of the ESR technique. The work reviewed in this chapter, and elsewhere in this volume, clearly shows that it can provide enhanced sensitivity and/or spectral resolution in many applications. Furthermore, it lends itself to a multi-frequency approach, which is particularly advantageous in studies of molecular dynamics, as well as in structural studies. The development of the necessary technologies has proceeded rapidly in recent years, and additional improvements may be expected which will further enhance the applicability and utility of ESR in general.

ACKNOWLEDGMENTS. I wish to especially thank Dr. Keith A. Earle for his critical reading and many suggestions that have improved this chapter. This work was supported by grants from NIH/NCRR, NIH/GM, and NSF.

REFERENCES

1 Lebedev, Ya.S., 1990. High-Frequency Continuous-Wave Electron Spin Resonance. *Modern Pulsed and Continuous Wave ESR*, (Eds. Kevan L, Bowman MK) Wiley, NY, 365-404.

2 Budil, D.E., Earle, K.A., Lynch, W.B., Freed, J.H., 1989. Electron Paramagnetic Resonance at 1 Millimeter Wavelengths. *Advanced EPR Applications in Biology and Biochemistry*, (Ed. Hoff A) Elsevier, Amsterdam, Ch. 8:307-340.

3 Freed, J.H., 2000. New Technologies in Electron Spin Resonance. *Ann. Rev. Phys. Chem.* **51**:655-689.

4 Borbat, P.P., Costa-Filho, A.J., Earle, K.A., Moscicki, J.K., Freed, J.H., 2001. Electron Spin Resonance in Studies of Membranes and Proteins. *Science* **291**:266-269.

5 Feher, G., Richards, P.L., 1967. Determination of the Zero Field Splitting "D" in Heme Chloride by Far-Infrared Spectroscopy. *Magnetic Resonance in Biological Systems*, (Eds. Ehrenberg A, Malmström BG, Vänngård T) Pergamon Press, NY, 141-144.

6 Brackett, G.C., Richards, P.L., Caughey, W.S., 1971. Far-Infrared Magnetic Resonance In Fe(III) And Mn(III) Porphyrins, Myoglobin, Hemoglobin, Ferrichrome-A, And Fe(III) Dithiocarbamates. *J. Chem. Phys.* **54**:4383-4401.

7 Champion, P.M., Sievers, A.L., 1980. Far infrared magnetic resonance of deoxyhemoglobin and deoxymyoglobin. *J. Chem. Phys.* **72**:1569-1582.

8 Grinberg, O.Ya., Dubinskii, A.A., Shuvalov, V.F., Oranskii, L.A., Kurochkin, V.I., Lebedev, Ya.S., 1976. Submillimeter ESR Spectroscopy of Free Radicals. *Dokl. Phys. Chem.* 230:923.

9 Lynch, B., Earle, K.A., Freed, J.H., 1988. A 1 Millimeter-Wave ESR Spectrometer. *Rev. Sci. Instr.* **59**:1345-1351.

10 Barra, A.L., Brunel, L.C., Robert, J.B., 1990. EPR Spectroscopy at Very High-Field. *Chem. Phys. Lett.* **165**:107-9.

11 Earle, K.A., Budil, D.E., Freed, J.H., 1996. Millimeter Wave Electron Spin Resonance Using Quasioptical Techniques. *Adv. in Magn. and Optical Res.* **19**: Ch. 3:253-323.

12 Goldsmith, P.F., 1998. *Quasioptical Systems: Gaussian Beam Quasioptical propagation and Applications.* NY: IEEE Press.

13 Haindl, E., Möbius, K., Oloff, H., 1985. 94 GHz Electron-Paramagnetic-Res Spectrometer With Fabry-Perot Resonator. *Z. Naturforsch.* **A40**:169-72.

14 Earle, K.A., Freed, J.H., 1999. Quasioptical Hardware for a Flexible FIR-EPR Spectrometer. *Appl. Magn. Res.* **16**:247-272.

15 Tannenwald, P.E., 1980. Far Infrared Heterodyne Detectors. *Intl. J. of IR and MM Waves.* **1**:159-73.

16 Lucas, C., Amingual, D., Chataud, J.P., 1994. Recent Developments In Low-Temperature Infrared Detectors. *J. Phys. IV Colloq.* **4**:177-82.

17 Nilges, M.J., Smirnov, A.I., Clarkson, R.B., Belford, R.L., 1999. Electron Paramagnetic Resonance W-band Spectrometer with a Low-Noise Amplifier. *Appl. Magn. Reson.* **16**:167-83.

18 Earle, K.A., Budil, D.E., Freed, J.H., 1993. 250 GHz EPR of Nitroxides in the Slow-Motional Regime: Models of Rotational Diffusion. *J. Phys. Chem.* **97**:13289-13297.

19 Earle, K.A., Moscicki, J,, Polimeno, A., Freed, J.H., 1997. A 250 GHz. ESR Study of *o*-terphenyl: Dynamic Cage Effects above T_c. *J. Chem. Phys.* **106**:9996-10015.

20 Earle, K.A., Moscicki, J., Polimeno. A., Freed, J.H., 1998. Response to "Comment on 'A 250 GHz ESR Study of *o*-terphenyl Dynamic Cage Effects above T_c". *J. Chem. Phys.* **109**:10525-10526.

21 Budil, D.E., Earle, K.A., Freed, J.H., 1993. Full Determination of the Rotational Diffusion Tensor by Electron Paramagnetic Resonance at 250 GHz. *J. Phys. Chem.* **97**:1294-1303.

22 Polimeno, A., Freed, J.H., 1995. Slow Motional ESR in Complex Fluids: The Slowly Relaxing Local Structure Model of Solvent Cage Effects. *J. Phys. Chem.* **99**:10995-11006.

23 Budil, D.E., Lee, S., Saxena, S., Freed, J.H., 1996. Non-Linear Least Squares Analysis of Slow-Motion EPR Spectra in One and Two Dimensions Using a Modified Levenberg-Marquardt Algorithm. *J. Magn. Res.* **A120**:155-189.

24 Rao, K.V.S., Polnaszek, C.F., Freed, J.H., 1977. ESR Studies of Anisotropic Ordering, Spin Relaxation, and Slow Tumbling in Liquid Crystalline Solvents, II. *J. Phys. Chem.* **81**:449-456.

25 Liang, Z.C., Freed, J.H., 1999. An Assessment of the Applicability of Multifrequency ESR to Study the Complex Dynamics of Biomolecules. *J. Phys. Chem. B* **103**:6384-96.

26 Barnes, J., Liang, Z., Mchaourab, H., Freed, J.H., Hubbell, W.L., 1999. A Multi-Frequency ESR Study of T4 Lysozyme Dynamics. *Biophys. J.* **76**:3298-3306.

27 Pilar, J., Labsky, J., Marek, A., Budil, D.E., Earle, K.A., Freed, J.H., 2000. Segmental Rotational Diffusion of Spin Labeled Polystyrene in Dilute Toluene Solution by 9 and 250 GHz ESR. *Macromolecules* **33**:4438-4444.

28 Liang, Z., Bobst, A.M., Keyes, R.S., Freed, J.H., 2000. An Electron Spin Resonance Study of DNA Dynamics Using the Slowly Relaxing Local Structure Model. *J. Phys. Chem. B* **104**:5372-5381.

29 Budil, D.E., Kolaszkowski, S.V., Perry, A., Valaprasad, C., Johnson, F., Strauss, P.R., 2000. Dynamics and Ordering in a Spin-Labeled Oligonucleotide Observed by 220 GHz Electron Paramagnetic Resonance. *Biophys. J.* **78**: 430-438.

30 Bennati, M., Gerfen, G.J., Martinez, G.V., Griffin, R.G., Singel, D.J., Millhauser, G.L., 1999. Nitroxide side-chain dynamics in a spin-labeled helix-forming peptide revealed by high-frequency (139.5-GHz) EPR spectroscopy. *J. Mag. Reson.* **139**:281-286.

31 Smirnov, A.I., Belford, R.L., Clarkson, R.B., 1998. Comparative spin label spectra at X-band and W-band. *Biol. Magn. Reson.* **14**:83-108.

32 Barnes, J.P., Freed, J.H., 1998. Dynamics and Ordering in Mixed Model Membranes of DMPC and DMPS: A 250 GHz. ESR Study. *Biophys. J.* **75**:2532-2546.

33 Marsh, D., Gaffney, B., 1998. High-Frequency, Spin-Label EPR of Nonaxial Lipid Ordering and Motion in Cholesterol-Containing Membranes. *Proc. Natl. Acad. Sci.* **95**:12940-43.

34 Lou, Y., Ge, M., Freed, J.H., 2001. A Multifrequency ESR Study of the Complex Dynamics of Membranes. *J. Phys. Chem. B* **105**:11053-11056.

35 Clarkson, R.B., Smirnov, A.I., Smirnova, T.I., Kang, H., Belford, R.L., Earle, K.A., Freed, J.H., 1998. Multi-Frequency EPR Determination of Zero-Field Splitting of High-Spin Species in Liquids: Gd (III) Chelates in Water. *Molec. Physics.* **95**:1325-1332.

36 Shin, D.H., Dye, J.L., Budil, D.E., Earle, K.A., Freed, J.H., 1993. 250 GHz and 9.5 GHz EPR Studies of an Electride and Two Alkalides. *J. Phys. Chem.* **97**:1213-1219.

37 Vanderdonk, W.A., Stubbe, J., Gerfen, G.J., Bellew, B.F., Griffin, R.G., 1995. EPR Investigations of the Inactivation of E. coli Ribonucleotide Reductase with 2'-Azido-2'-deoxyuridine 5'-Diphosphate: Evidence for the Involvement of the Thiyl Radical of C225-R1. *J. Am. Chem. Soc.* **117**:8908-8916.

38 Smirnova, T.I., Smirnov, A.I., Clarkson, R.B., Belford, R.L., Kotake, Y., Janzen, E.G., 1997. High-Frequency (95 GHz) EPR Spectroscopy To Characterize Spin Adducts. *J. Phys. Chem.* **B101**:3877-85.

39 vanderEst, A., Prisner, T., Bittl, R., Fromme, P., Lubitz, W., Möbius, K., Stehlik, D., 1997. Time-Resolved X-, K-, and W-Band EPR of the Radical Pair State $P_{700}^{\bullet+}A_1^{\bullet-}$ of Photosystem I in Comparison with $P_{865}^{\bullet+}Q_A^{\bullet-}$ in Bacterial Reaction Centers. *J. Phys. Chem. B* **101**:1437-43.

40 Tipikin, D.S., Earle, K.A., Freed, J.H., 1999. The High Frequency EPR Spectra of Polyaniline: Line Narrowing due to Spin Exchange. *Polymer Science.* **B 41**:1043-1047.

41 Clarkson, R.B., Wang, W., Brown, D.R., Crookham, H.C., Belford, R.L., 1990. Multifrequency EPR Studies of Argonne and Illinois Sample Bank Coals. *Fuel* **69:**1405-1411.

42 Earle, K.A., Moscicki, J.K., Ge, M., Freed, J.H., 1994. 250 GHz ESR Studies of Polarity Gradients along the Aliphatic Chains in Phospholipid Membranes. *Biophys. J.* **66:**1213-1221.

43 Lynch, W.B., Boorse, R.S., Freed, J.H., 1993. A 250 GHz ESR Study of Highly Distorted Manganese Complexes. *J. Am. Chem. Soc.* **115:**10909-10915.

44 Wood, R.M., Stucker, D.M., Jones, L.M., Lynch, W.B., Misra, S.K., Freed, J.H.1999. An EPR Study of Some Highly Distorted Tetrahedral Manganese (II) Complexes at 250 GHz. *Inorgan. Chem.* **38:**5384-5388

45 Policar, C., Knüpling, M., Frapart, Y.M., and Un, S., 1998. Multifrequency High-Field EPR Study of Binuclear Mn(III)Mn(IV) Complexes. *J. Phys. Chem. B* **102:** 10391-98.

46 Barra, A-L., Gatteschi, D., Sessoli, R., Abbati, G.L., Cornia, A., Fabretti, A.C., Uytterhoeven, M.G., 1999. Electronic structure of manganese(III) compounds from high-frequency EPR spectra. *Angew. Chemie,* **36:**2329-31.

47 Telser, J., Pardi, L.A., Krzystek, J., Brunel, C., 1998. EPR Spectra from "EPR-Silent" Species: High-Field EPR Spectroscopy of Aqueous Chromium(II). *Inorg. Chem.* **37:**5769-75.

48 Misra, S.K., Andronenko, S.A., Earle, K.A., Freed, J.H., 2001. Single-Crystal EPR Studies of Transition-Metal Ions in Inorganic Crystals at Very High Frequencies. *Appl. Magn. Res.* **21:** 549-561.

49 Misra, S.K., Andronenko, S.I., Rinaldi, G., Chard, P., Earle, K.A., Freed, J.H., 2003. Variable-Frequency EPR Study of Mn^{2+}-doped $NH_4Cl_{0.9}I_{0.1}$Single Crystal at 9.6, 36 and 249.9 GHz: Structural Phase Transition. *J. Magn. Res.* **160:**131-138.

50 Barnes, J.P., Freed, J.H., 1997. Aqueous Sample Holders for High-Frequency ESR. *Rev. Sci. Instrum.* **68:**2838-2846.

51 Barnes, J.P., Freed, J.H., 1998. A Shunt Fabry-Perot Resonator for High Frequency ESR Using a Variable Coupling Scheme. *Rev. Sci. Instrum.* **69:**3022-3027.

52 Earle, K.A., Tipikin, D.S., Freed, J.H., 1996. Far Infrared EPR Spectrometer Utilizing a Quasi-Optical Reflection Bridge. *Rev. Sci. Instr.* **67:**2502-2513.

53 Smith, G.M., Le Surf, J.C.G., Mitchell, R.H., Riedi, P.C., 1998. Quasi-optical cw mm-wave electron spin resonance spectrometer. *Rev. Sci. Instrum.* **69:**3924-3927.

54 Budil, D.E., Ding, Z., Smith, G.R., Earle, K.A., 2000. Jones Matrix Formalism for Quasioptical EPR. *J. Magn. Res.* **144:**20-34.

55 Hassam, A.K., Maniero, A-L., van Tol, H., Saylor, C., Brunel, L.C., 1999. High-Field EMR: Recent Developments at 25 Tesla, and Next-Millenium Challenges. *Appl. Magn. Res.* **16:** 299-308.

56 Cardin, J.T., Kolaczkowski, S.V., Anderson, S.V., Budil, D.E., 1999. Quasioptical Design for an EPR Spectrometer Based on a Horizontal-Bore Superconducting Solenoid. *Appl. Magn. Res.* **16:**273-292.

57 Fuchs, M.R., Prisner, T,R,, Möbius, K., 1999. A high-field/high-frequency heterodyne induction-mode electron paramagnetic resonance spectrometer operating at 360 GHz. *Rev. Sci. Instrum.* **70:**3681-3.

58 Hassan, A., van Tol, J., Maniero, A.L., Brunel, L.C., Earle, K.A., Freed, J.H., 1999. Study of Motional Dynamics in Complex Fluids by Very High-Field, Very High-Frequency EPR (VHF-EPR). *Physical Phenomena at High Magnetic Fields-III*. Eds. Z. Fisk, L. Gurkov, J. R. Schrieffer, World Scientific Publishers, NJ, 453-456.

59 Prisner, T.F., 1997. Pulsed high-frequency/high-field EPR. *Adv. in Magn. and Optical Res.* **20**:245-300.

60 Allgeier, J., Disselhorst, J.A.J.M., Weber, R.T., Wenckebach, W.T., Schmidt, J., 1990. High-Frequency Pulsed Electron Spin Resonance. in *Modern Pulsed and Continuous Wave ESR,* Eds. L. Kevan, and M.K. Bowman, Wiley, NY, 267-284.

61 Bresgunov, A.Y., Dubinskii, A.A., Krymov, V.N., Petrov, Y.G., Poluektov, O.G., Lebedev, Y.S., 1991. Pulsed EPR in 2-mm Band. *Appl. Magn. Res.* **2**:715.

62 Bennati, M., Farrar, C.T., Bryant, J.A., Inati, S.J., Weis, V., Gerfen, G.J., Riggs-Gelasco, P., Stubbe, J., Griffin, R.G., 1999. Pulsed Electron-Nuclear Double Resonance (ENDOR) at 140 GHz. *J. Magn. Res.* **138**:232-243.

63 Rohrer, M., Gast, P., Möbius, K., Prisner, T.F., 1996. Anisotropic motion of semiquinones in photosynthetic reaction centers of *Rhodobacter sphaeroides* R26 and in frozen isopropanol solution as measured by pulsed high-field EPR at 95 GHz. *Chem. Phys. Lett.* **259**:523-30.

64 Gromov, I., Krymov, V., Manikandan, P., Arieli, D., Goldfarb, D., 1999. A W-Band Pulsed ENDOR Spectrometer: Setup and Application to Transition Metal Centers. *J. Magn. Res.* **139**:8-17.

65 Weis, V., Bennati, M., Rosay, M., Bryant, J.A., Griffin, R.G., 1999. High-Field DNP and ENDOR with a Novel Multiple-Frequency Resonance Structure. *J. Magn. Res.* **140**:293-299.

66 Calame, J.P., Danly, B.G., Garven, M., 1999. Measurements of intrinsic shot noise in a 35 GHz gyroklystron. *Physics of Plasmas* **6**:2614-2925.

67 Moll, H.P., Kutter, C., van Tol, J., Zuckerman, H., Wyder, P., 1999. Principles and Performance of an Electron Spin Echo Spectrometer Using Far Infrared Lasers as Excitation Sources. *J. Magn. Res.* **137**:46-58 .

68 Hofbauer, W., Earle, K.A., Dunnam, C., Freed, J.H., A High Power 95 GHz Pulsed ESR Spectrometer. (to be published).

69 Mead, J., McIntosh, R., 1991. Pulsed polarimetric millimeter-wave radars that utilize extended interaction amplifier and oscillator tubes. *Nat'l. Telesystems Conf. Proc.* **1**:343-6.

70 Blank, M., Danly, B.G., Levush, B., Calame, J.P., Nguyen, K., Pershing, D., Petillo, J., Hargreaves, T.A., True, R.B., Theiss, A.J., Good, G.R., Felch, K., James, B.G., Borchard, P., Cahalan, P., Chu, T.S., Jory, H., Lawson, W.G., Antonsen, T.M. Jr., 1999. Demonstration of a 10 kW average power 94 GHz gyroklystron amplifier.*Physics of Plasmas* **6**:4405-9.

71 Dumesh, B.S., Surin, L.A., 1996. Two highly sensitive microwave cavity spectrometers. *Rev. Sci. Instrum.* **67**:3458-64.

72 Risaliti, R., Ronchi, L., Scordino, A., 1988. Modified Ledatron And Orotron Tubes With Improved Sub-mm Performance. *Infrared Phys.* **28**:353-61.